Studies of *Pseudomonas aeruginosa* Azurin Mutants: Cavities in β-Barrel Do Not Affect Refolding Speed

Irina Pozdnyakova, Jesse Guidry, and Pernilla Wittung-Stafshede
Department of Chemistry, Tulane University, New Orleans, Louisiana 70118 USA

ABSTRACT   *Pseudomonas aeruginosa* azurin is a blue-copper protein with a Greek-key fold. Removal of copper produces an apoprotein with the same structure as holoazurin. To address the effects on thermodynamic stability and folding dynamics caused by small cavities in a β-barrel, we have studied the behavior of the apo-forms of wild-type and two mutant (His-46-Gly and His-117-Gly) azurins. The equilibrium- and kinetic-folding and unfolding reactions appear as two-state processes for all three proteins. The thermodynamic stability of the two mutants is significantly decreased as compared with the stability of wild-type azurin, in accord with cavities in or near the hydrophobic interior having an overall destabilizing effect. Large differences are also found in the unfolding rates: the mutants unfold much faster than wild-type azurin. In contrast, the folding-rate constants are almost identical for the three proteins and closely match the rate-constant predicted from the native-state topology of azurin. We conclude that the topology is more important than equilibrium stability in determining the folding speed of azurin.

INTRODUCTION

Many small proteins fold by two-state mechanisms, whereas proteins of larger size often have complex folding transitions involving intermediates (Jackson, 1998). For small proteins folding with two-state kinetics, parameters such as sequence, size, thermodynamic stability, and topology may affect the protein-folding rates to various extents. A recent study identified a statistically significant correlation between the native-state topology and the folding speed for a large set of small, unrelated proteins (Plaxco et al., 1998). It was shown that proteins with structures containing mainly local interactions (such as α-helices) have rapid folding transitions, whereas proteins with structures including more long-range contacts (such as β-sheets) usually fold more slowly. In addition, for homologous proteins with the same topology, thermodynamic stability appears to further dictate the folding rate (Plaxco et al., 1998).

Until recently, folding studies of proteins with β-sheet structure have been sparse (Capaldi and Radford, 1998; Carlsson and Jonsson, 1995). The folding pathways of β-sheet proteins may differ significantly from those of helical- and mixed α/β-proteins because the interactions that stabilize β-sheet proteins are predominantly nonlocal in nature. Theoretical models predict that β-sheet formation is initiated at β-hairpin structures (Finkelstein, 1991). Sheet propagation is believed to occur by addition of further strands. The rate-limiting step in β-sheet formation was proposed to be the formation of a few specific interactions within the first β-hairpin (Finkelstein, 1991; Schonbrunner et al., 1997; Eaton et al., 1996). Recent kinetic studies of

proteins such as Src homology (SH3) domains, fibronectin type III domains, tendamistat, and cold-shock proteins have shown that folding of β-sheet proteins can occur with and without intermediates, with fast and slow refolding rates, and late to very late transition states (Capaldi and Radford, 1998).

Azurin is a good model for studies of β-sheet formation. It is a small protein that belongs to the class of blue-copper proteins (Adman, 1991) and functions as an electron carrier in bacterial respiration. Azurin has a β-barrel structure arranged in a double-wound Greek-key topology (Adman, 1991). The intense blue color of azurin is due to an absorbance at 625 nm originating from sulfur-to-copper charge-transfer (Adman, 1991). In *Pseudomonas aeruginosa* azurin (Nar et al., 1992a,b), the copper is coordinated by three strong ligands arranged in a trigonal-planar configuration: the side-chains of Cys-112, His-117, and His-46. At the axial positions, the copper weakly interacts with the sulfur of Met-121 and the carbonyl oxygen of Gly-45. The crystal structures of copper-, zinc-, and apo-azurin have all been determined with high resolution (Adman, 1991; Nar et al., 1992a,b). There is no significant structural difference between the proteins, confirming that azurin adopts a native β-barrel structure also with an empty metal-site. Azurin contains one buried tryptophan that gives rise to a strong fluorescence signal at 308 nm in the folded (apo) state (Gilardi et al., 1994).

The mutations His-117-Gly (histidine-to-glycine mutation at position 117) and His-46-Gly (histidine-to-glycine mutation at position 46) were initially implemented in *P. aeruginosa* azurin to study reconstitution of the type-1 copper site by addition of exogenous ligands (den Blaauwen et al., 1993; van Pouderoyen et al., 1996; Hammann et al., 1997). Because the imidazole ring of His-117 protrudes through the surface of the protein, replacing His-117 by glycine creates a channel leading from the bulk solvent directly to the hydrophobic core (Fig. 1). His-46, on the
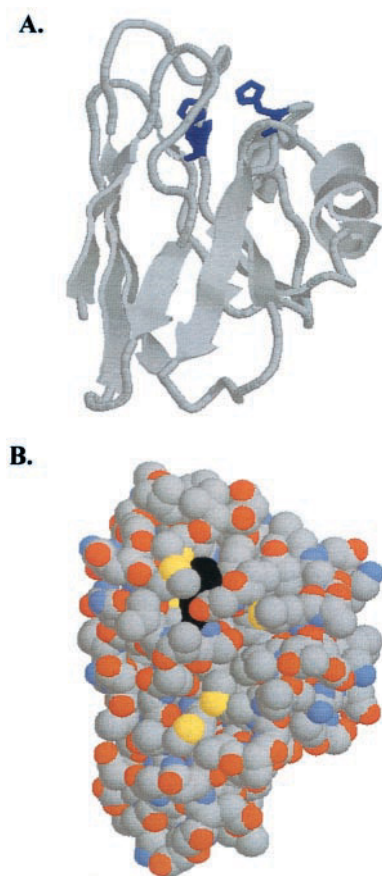
FIGURE 1 Schematic structure of *P. aeruginosa* azurin (1azu.pdb). (*A*) Backbone diagram with His-117 (to the *right*) and His-46 (to the *left*) shown in blue stick representation. (*B*) Space-fill representation with His-117 shown in black color. In contrast, His-46 is not visible from the surface of the protein (note that the view in *B* is rotated with respect to that presented in *A*).

other hand, is buried inside the protein and mutating this histidine into glycine produces a cavity inside the protein. In both cases crystallographic studies showed that the mutations did not induce perturbations of the overall β-barrel structure, and the introduced cavities were found to contain water-molecules (Hammann et al., 1997).

To address the effects on stability and folding dynamics caused by cavities in or near the core of a β-barrel, here we report a comparative study on the apo-forms of wild-type, His-117-Gly and His-46-Gly *P. aeruginosa* azurins. We find that the mutations dramatically decrease the equilibrium stability of azurin. Time-resolved experiments reveal apparent two-state kinetic folding and unfolding processes for all three variants. The folding speed in water is very similar for wild type, His-117-Gly and His-46-Gly azurins, whereas unfolding proceeds much more rapidly for the two mutants. The experimental folding rates in water are accurately matched by the rate predicted from azurin's native-state structure. Hence, native-state topology, and not equi-

librium stability, is the most important determinant of the formation speed of azurin's β-barrel.

MATERIALS AND METHODS

Protein expression and purification

Plasmids (pUC18 derivatives) carrying wild-type, His-117-Gly, and His-46-Gly point-mutated azurin sequences were generous gifts from Dr. G. Karlsson (University of Gothenburg, Sweden). Proteins were expressed in *Escherichia coli* strain RV308; purification was performed as described previously but with a few changes (Karlsson et al., 1989; Leckner et al., 1997; Pozdnyakova et al., 2001b). Briefly, cell paste was equilibrated in a sucrose buffer (20% Tris-buffer, pH 8) and subjected to osmotic shock (0.5 mM MgCl$_2$) resulting in a periplasmic preparation. Protein precipitation by decreasing the pH to 4.1 (50 mM NH$_3$-acetate buffer) yielded an azurin-containing supernatant that was loaded onto a SP Sepharose column (Pharmacia Biotech, Piscataway, NJ); azurin was eluted by a pH gradient (from 4.1 to 9.0, using 50 mM NH$_3$-acetate buffer). After polyethylene glycol dialysis, gel filtration on a Superdex 75 (Pharmacia Biotech) column yielded pure (as verified by gel electrophoresis) apoprotein. No copper was added during cell-growth or purification. In the case of the wild-type preparation, zinc-bound azurin was separated from the apoprotein in the pH-gradient on the SP Sepharose column (zinc and apo azurin have different isoelectric points). Zinc did not bind to the two mutant forms of azurin. Apoprotein was verified, for all three proteins, by copper titration.

Equilibrium unfolding reactions

GuHCl-induced unfolding experiments (10–100 μM protein) were performed in 5 mM phosphate, pH 7.0, 20°C (using ultra pure GuHCl from Sigma, St. Louis, MO). Absorption, fluorescence (285-nm excitation), and far-ultraviolet circular dichroism (CD) were measured on Cary 50, Cary Eclipse, and OLIS instruments, respectively. For copper-titrations (to verify apoprotein), Cu^{2+} was added as CuSO$_4$. GuHCl-induced unfolding was reversible in all cases, and there was no protein-concentration dependence for the transitions (Pozdnyakova et al., 2001a,b). The transitions were analyzed using a two-state model (Pozdnyakova et al., 2001a,b) to determine $\Delta G_U(H_2O)$ and m values. The transition-midpoints were calculated as $\Delta G_U(H_2O)/m$ or by direct inspection of the transitions.

Folding and unfolding kinetics

Time-resolved folding and unfolding measurements were carried out on an Applied Photophysics (Leatherhead, UK) SX.18MV stopped-flow reaction analyzer in fluorescence mode (excitation at 285 nm; emission detected at 308 nm). Wild-type, His-117-Gly, and His-46-Gly apoazurin proteins were mixed in 1:5 or 1:10 ratios with appropriate GuHCl/buffer solutions. A minimum of six kinetic traces were averaged and fit to monophasic decay equations using a nonlinear least-squares algorithm supplied by Applied Photophysics. There was no burst phase in either the folding or unfolding kinetics (instrument deadtime: 4–6 ms). The unfolding and refolding rate constants at different denaturant concentrations were fit in KaleidaGraph assuming standard linear dependence of ln k_F and ln k_U on GuHCl concentration (Fersht, 1997):

$$\ln k = \ln[k_F(H_2O)\exp(m_F[GuHCl]/RT)$$

$$+ k_U(H_2O)\exp(m_U[GuHCl]/RT)]$$

In this equation, m_U is the slope of the unfolding branch, and m_F is the slope of the folding branch. $k_F(H_2O)$ and $k_U(H_2O)$ are the folding and unfolding rate constants in aqueous solution (i.e., in absence of GuHCl).
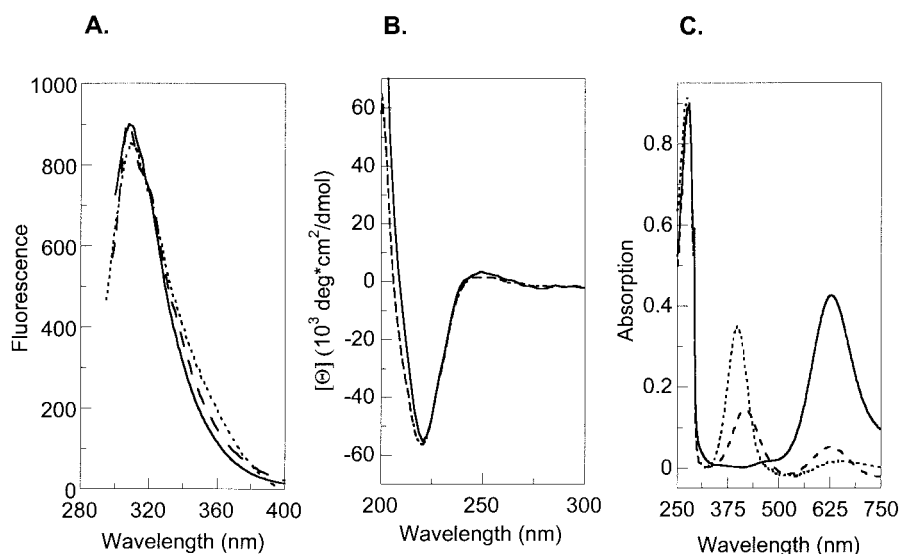
FIGURE 2 Tryptophan fluorescence (*A*), far-UV CD (mean residue elipticity) (*B*), and visible absorption (*C*), the latter upon Cu(II) addition, spectra for native forms of wild-type (*solid lines*), His-117-Gly (*dashed lines*), His-46-Gly (*dotted lines*) apoazurins.

RESULTS

Native structure of azurin mutants

The His-117-Gly and His-46-Gly mutants adopt structures that are identical to the structure of wild-type azurin (den Blaauwen et al., 1993; van Pouderoyen et al., 1996; Hammann et al., 1997). For each apomutant prepared by us, copper addition produces an electronic spectrum identical to that reported in the literature: absorption maxima observed at 420 and 628 nm for His-117-Gly azurin and at 400 nm (with weaker bands at 630 and 760 nm) for His-46-Gly azurin. This excludes the presence of cysteine-sulfur oxidation in the apoproteins since the cysteine-modified form of the proteins cannot bind copper. Mass-spectroscopy analysis also confirmed that no modification took place. In Fig. 2, far-ultraviolet (UV) CD, tryptophan emission, and visible absorption, the latter upon copper-addition, spectra for the native forms of wild-type, His-117-Gly, and His-46-Gly azurins are shown. It is clear from the presented data that all three apoproteins adopt identical β-barrel structures in solution.

Equilibrium unfolding of wild-type, His-117-Gly, and His-46-Gly azurins

Unfolding of apoazurin can be monitored by far-UV CD (the negative β-sheet band at 220 nm disappears upon unfolding) and by tryptophan (tryptophan-48) emission (the emission decreases upon unfolding due to increased solvent exposure). GuHCl-induced equilibrium unfolding of the apoforms of wild-type, His-117-Gly and His-46-Gly azurins have been reported earlier (Pozdnyakova et al., 2001a,b) but not compared. All three proteins unfold in sharp transitions (Fig. 3;

data adapted from Pozdnyakova et al., 2001a,b). The thermodynamic stability is significantly decreased for the mutants as compared with wild-type azurin: unfolding midpoints are observed at 1.1, 1.2, and 1.7 M GuHCl for His-46-Gly, His-117-Gly, and wild-type azurin, respectively (Table 1).

Applying two-state approximations to the unfolding data, free-energies of unfolding in absence of denaturant, $\Delta G_U(H_2O)$, of 18.2($\pm$0.9) kJ/mol for His-46-Gly and 19.2 ($\pm$0.6) kJ/mol for His-117-Gly azurin can be derived (Pozdnyakova et al., 2001b). The $\Delta G_U(H_2O)$ for wild-type apoa-
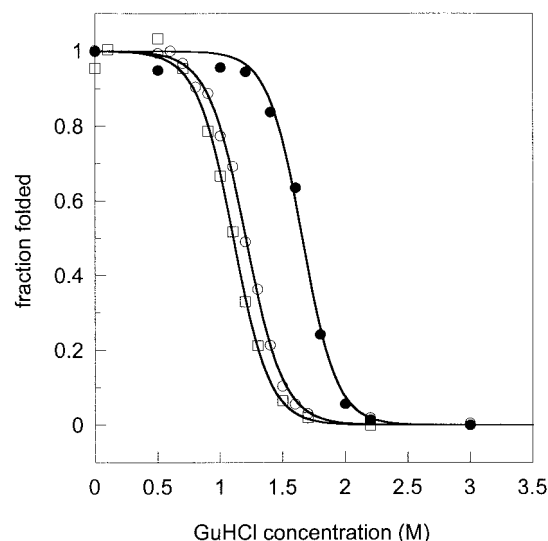

FIGURE 3 Equilibrium unfolding of wild-type ($\bullet$), His-117-Gly ($\circ$), His-46-Gly ($\square$) apoazurins as a function of GuHCl concentration (data taken from Pozdnyakova et al., 2001a,b). Solid lines represent two-state fits (Table 1).

TABLE 1 Thermodynamic unfolding parameters for wild-type, His-117-Gly, and His-46-Gly azurin

Azurin variant	Wild type	His-117-Gly	His-46-Gly
$[GuHCl]_{1/2}$	1.7 M	1.2 M	1.1 M
$\Delta G_U(H_2O)_{eq}$	29.1 ($\pm$2.3) kJ/mol	19.2 ($\pm$0.6) kJ/mol	18.2 ($\pm$0.9) kJ/mol
m_{eq}	17.5 ($\pm$1.4) kJ/mol, M	16.0 ($\pm$0.5) kJ/mol, M	16.5 ($\pm$0.8) kJ/mol, M
$\Delta[\Delta G_U(H_2O)_{eq}]$	—	10 ($\pm$3) kJ/mol	11 ($\pm$3) kJ/mol
$\ln k_F(H_2O)$	4.9 ($\pm$0.3)	4.3 ($\pm$0.3)	4.1 ($\pm$0.3)
$\ln k_U(H_2O)$	-4.3 ($\pm$1.0)	-1.3 ($\pm$1.0)	-1.2 ($\pm$1.0)
$\Delta[RT \ln k_U(H_2O)]$	—	7 ($\pm$3) kJ/mol	8 ($\pm$3) kJ/mol
$m_F/(m_F - m_U)$	0.60 ($\pm$0.04)	0.5 (0.1)	0.4 (0.1)

zurin is much higher: 29 ($\pm$2.3) kJ/mol (Table 1). The m_{eq} values (measure of hydrophobic-surface area exposed upon unfolding (Pace, 1975; Tanford, 1970)) are similar for the three proteins, (16–17 kJ/mol, M; Table 1), in accord with identical well-packed, folded structures.

Time-resolved folding dynamics

Folding and unfolding kinetics were investigated by monitoring changes in the tryptophan-emission upon stopped-flow mixing. Both processes appear monoexponential for all three proteins (examples shown in Fig. 4), and there is no missing amplitude within the instrument dead time. The kinetic data produces a V-shaped curve when the logarithm of the rate constants are plotted as a function of GuHCl concentration (a so-called Chevron plot (Fersht, 1997), Fig. 5). A preliminary study of His-117-Gly apoazurin folding dynamics was reported earlier (Pozdnyakova et al., 2001b). We note that the results therein are not in full agreement with those presented here (the unfolding midpoint derived from the earlier kinetic data differs significantly). However, the current data set is larger and, therefore, more reliable. Applying two-state fits

(see Materials and Methods) to the kinetic data, the folding-rate constants for wild-type, His-117-Gly and His-46-Gly azurins in absence of denaturant, $k_F(H_2O)$, were determined to be 140 ($\pm$50) s^{-1}, 70 ($\pm$30) s^{-1}, and 60 ($\pm$20) s^{-1}, respectively (Table 1). Because folding rate constants for different proteins can vary more than six orders of magnitude (Plaxco et al., 1998), the rates measured here can be considered, within errors, to be identical. The variation in $\ln k_F(H_2O)$ is between 4.1 and 4.9. In sharp contrast, the unfolding rates are significantly different from each other ($\ln k_U(H_2O)$ varies between -1.2 and -4.3). The two mutants unfold much more rapidly than wild-type azurin at all denaturant conditions (Fig. 5). At 0 M GuHCl, the increases in unfolding rate constants for His-117-Gly and His-46-Gly as compared with the unfolding rate for wild-type azurin, $\Delta[RT \ln k_U(H_2O)]$ of 7 and 8 kJ/mol, correspond to the majority ($\sim$70–80%) of the equilibrium-unfolding free-energy differences, $\Delta[\Delta G_U(H_2O)_{eq}]$ of 10 and 11 kJ/mol (Table 1).

In accord with two-state kinetic processes, the $\Delta G_U(H_2O)$ values for wild-type, His-117-Gly, and His-46-Gly apoazurins calculated from kinetic data, $\Delta G_U(H_2O) = RT \ln(k_F/k_U)$ of 23
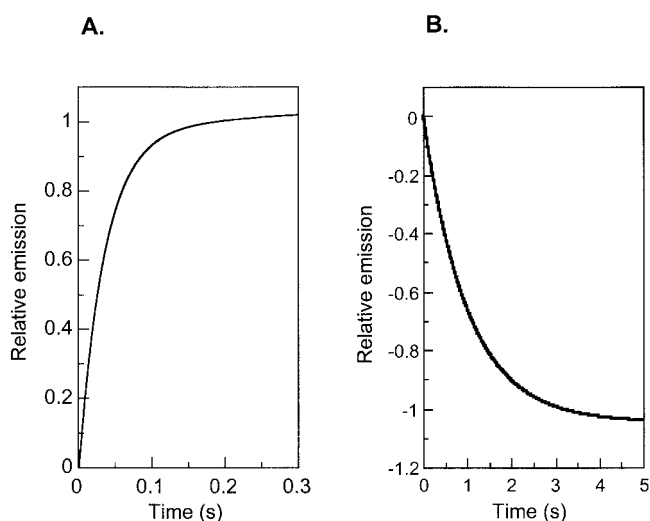
A.

B.

FIGURE 4 Examples of refolding- and unfolding-kinetic traces detected upon stopped-flow mixing. (*A*) Wild-type azurin refolding kinetics in 0.9 M GuHCl. (*B*) Wild-type azurin unfolding kinetics in 2.5 M GuHCl.
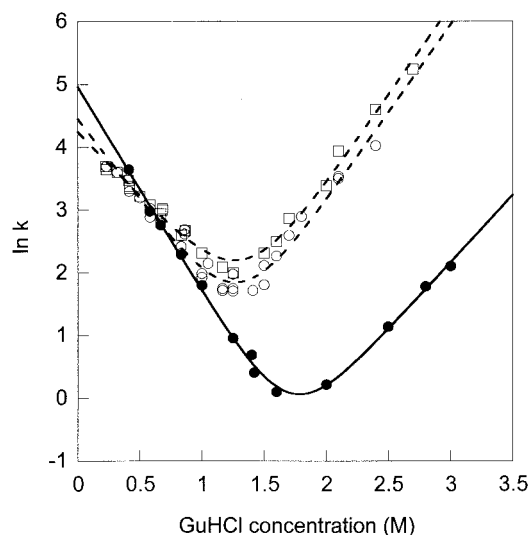

FIGURE 5 Natural logarithm of folding- and unfolding-rate constants as a function of GuHCl concentration (ln k versus GuHCl) for wild-type ($\bullet$), His-117-Gly ($\circ$), and His-46-Gly ($\square$) apoazurins. Solid and dashed lines are two-state fits (see Table 1 and text).

(±4), 14 (±5), and 13 (±5) kJ/mol, are in rough agreement (within 25%) with the values derived in the equilibrium-unfolding experiments ($\Delta G_U(H_2O)_{eq}$ of 29 (±3), 19 (±1), and 18 (±1) kJ/mol, respectively). The parameter $m_F/(m_F - m_U)$ gives an estimate for the relative amount of surface area buried in the transition state for folding as compared with the unfolded and folded states. For wild-type azurin this factor is 0.60 (±0.04), which corresponds to a rather native like, and therefore highly organized, folding-transition state. The folding-transition states in the two mutants appear somewhat less ordered as compared with that of wild-type azurin ($m_F/(m_F - m_U)$ 0.4–0.5 for the mutants; see Table 1).

DISCUSSION

Replacing His-117 in azurin by a glycine creates a channel leading from the bulk solvent directly to the interior core. His-46, on the other hand, is buried inside azurin and mutating this histidine into a glycine produces a cavity inside the protein (Fig. 1). The His-117-Gly and His-46-Gly azurin mutants adopt native-like structures that have been well characterized (den Blaauwen et al., 1993; van Pouderoyen et al., 1996; Hammann et al., 1997; Jeuken et al., 2000). Hence, these mutants are useful for investigations of the effects on thermodynamic stability and formation speed upon introducing cavities near, or in, the hydrophobic core of a β-barrel.

Effect of mutations on equilibrium stability

Wild-type (Pozdnyakova et al., 2001a) and the two mutant (Pozdnyakova et al., 2001b) azurins all unfold reversibly in apparent two-state processes (Fig. 3). Although the mutated histidines do not involve hydrophobic interactions in wild-type azurin, their removal (at either position 117 or 46) nevertheless creates cavities within the hydrophobic core of the β-barrel. We find the thermodynamic stability to be largely decreased for the mutants ($\Delta G_U(H_2O)$ of 18 to 19 kJ/mol as compared with 29 kJ/mol for wild type). The empty space created by removal of the imidazole side chain in each mutant is occupied by several water molecules (Hammann et al., 1997), suggesting that azurin's stability is decreased when extra water molecules are trapped in, or near, the hydrophobic core. Studies of other cavity-forming mutant proteins have shown that an interior cavity often destabilizes the protein (Buckle et al., 1996). A recent report (Takano et al., 1997), that addressed the issue of buried water molecules, concluded that water molecules stabilize engineered cavity-containing proteins with respect to the stability of the mutant protein with an empty cavity; however, the water-containing mutants were still less stable than the wild-type protein. It is also possible that at least some of the observed decrease in stability for the mutants (as compared with wild type) arise from increased entropy in the unfolded and/or folded states, because a glycine will have more degrees of freedom than a histidine. Nuclear magnetic resonance studies have shown that the dynamics in the mutated area of His-117-Gly azurin is increased, whereas the more rigid part of the protein framework, i.e., the β-barrel, is not disturbed by the mutation (Jeuken et al., 2000). In active azurin, His-117 and His-46 are exclusively involved in copper coordination. Upon copper removal, these residues instead coordinate a water molecule that replaces the copper. Inspection of the crystal structure of apoazurin suggests that there are no favorable interactions between the two histidines and other residues that may (if present) contribute to the higher thermodynamic stability of the wild-type protein as compared with the mutants lacking the histidines.

Insights into β-barrel formation

Folding and unfolding of the three apoproteins occur in apparent two-state reactions without kinetic intermediates (Fig. 4). Strikingly, the folding-rate constants are almost identical for the three proteins, whereas significant differences are found in the unfolding rates (Fig. 5). The two mutants unfold much more rapidly than the wild-type protein. In each case, the decrease in equilibrium stability is 70 to 80% accounted for in the increased unfolding-rate constant (Table 1). We conclude, therefore, that the eliminated residues (His-46 and His-117) do not form important contacts in the transition-state for folding; instead they appear to adopt native-like interactions only after the rate-limiting step. It was shown for a family of immunoglobin proteins, that have a Greek-key topology like azurin, that the transition state for folding involved a large fraction of the core residues with the N and C termini unrestrained (Hamill et al., 2000). The folding-transition state for azurin involves burial of ~60% of the hydrophobic-surface area of the native state (Table 1). Therefore, in analogy with the immunoglobin-like proteins, formation of an extended set of hydrophobic-core interactions is probably rate limiting during azurin folding. The mutated residues are not directly in the core of the azurin β-barrel (Fig. 1). His-117 is positioned on the protein surface, and it is near the C terminus in the primary structure. Although His-46 is almost in the center of the primary structure, and within the barrel in the tertiary structure, its side chain extends to the surface of the folded protein.

For the predominantly β-sheet protein tendamistat, sheet formation was shown to nucleate from a specific β-hairpin (Schonbrunner et al., 1997). Also theoretical calculations and kinetic-peptide studies have suggested β-hairpins as the initiation sites for formation of larger β-sheet structures (Finkelstein, 1991; Eaton et al., 1996). In the case of azurin, we have speculated that a C-terminal polypeptide segment incorporating three copper

ligands, adopting a β-hairpin structure in folded azurin, is the nucleation site for folding (Pozdnyakova et al., 2000). Support for this suggestion comes from the finding that a small peptide corresponding to this part of azurin specifically binds copper and, upon binding, adopts β-structure. It is possible that the β-hairpin is formed in the unfolded state of full-length azurin and acts as a folding nucleus. Replacing His-117 with a glycine adds more flexibility in the hairpin region. Thus, if the presence of the hairpin is important for nucleation of folding, a slower folding rate for His-117-Gly, as compared with wild-type azurin is expected. There is, however, no significant difference in the folding speeds of His-117-Gly and wild-type azurins and we conclude that the C-terminal β-hairpin does not initiate apoazurin folding.

Topology as folding-speed determinant

The parameter contact order, defined as the normalized average sequence separation between interacting residues in the folded state (Plaxco et al., 1998) is a measure of local versus long-range interactions in the native-state structure. The observed correlation between native-state contact order and protein-folding speed (Plaxco et al., 1998) for unrelated proteins was recently explained in terms of an extended nucleus with native-like topology in the transition-state for folding (Fersht, 2000). The contact order for native azurin is 16.7% (Pozdnyakova et al., 2001b). In this calculation, copper interactions are not included and, thus, the contact-order estimate is for the apo form. The contact order for wild-type apoazurin corresponds to a predicted folding-rate constant of 62 s^{-1}(ln k_F = 4.1). If the eliminated histidine side-chains in the mutants contribute to the contact order of wild-type azurin (through close contacts with other protein residues), the contact-order will be different for the mutants. This is however not the case for His-117-Gly and His-46-Gly azurins. The contact-order for azurin with His-117 and His-46 removed is different from that of wild-type azurin by only 0.4%, which corresponds to a change in predicted folding speed of 7% (which is negligible) (K. Plaxco, personal communication). There is an excellent agreement between the predicted folding-rate constant and our experimentally determined rate constants for the three azurin variants (60–140 s^{-1}, i.e., ln k_F of 4.1 to 4.9; Table 1), considering that folding rates of unrelated proteins can vary six orders of magnitude (Plaxco et al., 1998). Because the equilibrium stability largely differs among the three proteins, we conclude that native topology is the most important determinant of the formation speed of this β-barrel. Nevertheless, as a secondary determinant, thermodynamic stability further tunes the folding rates, since the less stable mutants fold slightly slower than wild-type azurin.

REFERENCES

Adman, E. T. 1991. Copper protein structures. *Adv. Protein Chem.* 42: 145–97.

Buckle, A. M., P. Cramer, and A. R. Fersht. 1996. Structural and energetic responses to cavity-creating mutations in hydrophobic cores: observation of a buried water molecule and the hydrophilic nature of such hydrophobic cavities. *Biochemistry.* 35:4298–4305.

Capaldi, A. P., and S. E. Radford. 1998. Kinetic studies of beta-sheet protein folding. *Curr. Opin. Struct. Biol.* 8:86–92.

Carlsson, U., and B. H. Jonsson. 1995. Folding of beta-sheet proteins. *Curr. Opin. Struct. Biol.* 5:482–487.

den Blaauwen, T., C. W. Hoitink, G. W. Canters, J. Han, T. M. Loehr, and J. Sanders-Loehr. 1993. Resonance Raman spectroscopy of the azurin His117Gly mutant: interconversion of type 1 and type 2 copper sites through exogenous ligands. *Biochemistry.* 32:12455–12464.

Eaton, W. A., P. A. Thompson, C. K. Chan, S. J. Hage, and J. Hofrichter. 1996. Fast events in protein folding. *Structure.* 4:1133–1139.

Fersht, A. R. 1997. Nucleation mechanisms in protein folding. *Curr. Opin. Struct. Biol.* 7:3–9.

Fersht, A. R. 2000. Transition-state structure as a unifying basis in protein-folding mechanisms: contact order, chain topology, stability, and the extended nucleus mechanism. *Proc. Natl. Acad. Sci. U. S. A.* 97:1525–1529.

Finkelstein, A. V. 1991. Rate of beta-structure formation in polypeptides. *Proteins.* 9:23–27.

Gilardi, G., G. Mei, N. Rosato, G. W. Canters, and A. Finazzi-Agro. 1994. Unique environment of Trp48 in *Pseudomonas aeruginosa* azurin as probed by site-directed mutagenesis and dynamic fluorescence spectroscopy. *Biochemistry.* 33:1425–1432.

Hamill, S. J., A. Steward, and J. Clarke. 2000. The folding of an immunoglobulin-like Greek key protein is defined by a common-core nucleus and regions constrained by topology. *J. Mol. Biol.* 297:165–178.

Hammann, C., G. van Pouderoyen, H. Nar, F. X. Gomis Ruth, A. Messerschmidt, R. Huber, T. den Blaauwen, and G. W. Canters. 1997. Crystal structures of modified apo-His117Gly and apo-His46Gly mutants of *Pseudomonas aeruginosa* azurin. *J. Mol. Biol.* 266:357–366.

Jackson, S. E. 1998. How do small single-domain proteins fold? *Fold. Des.* 3:R81–R91.

Jeuken, L. J., M. Ubbink, J. H. Bitter, P. van Vliet, W. Meyer-Klaucke, and G. W. Canters. 2000. The structural role of the copper-coordinating and surface-exposed histidine residue in the blue copper protein azurin. *J. Mol. Biol.* 299:737–755.

Karlsson, B. G., T. Pascher, M. Nordling, R. H. Arvidsson, and L. G. Lundberg. 1989. Expression of the blue copper protein azurin from *Pseudomonas aeruginosa* in *Escherichia coli*. *FEBS Lett.* 246:211–217.

Leckner, J., N. Bonander, P. Wittung-Stafshede, B. G. Malmstrom, and B. G. Karlsson. 1997. The effect of the metal ion on the folding energetics of azurin: a comparison of the native, zinc and apoprotein. *Biochim. Biophys. Acta.* 1342:19–27.

Nar, H., R. Huber, A. Messerschmidt, A. C. Filippou, M. Barth, M. Jaquinod, M. van de Kamp, and G. W. Canters. 1992a. Characterization and crystal structure of zinc azurin, a by-product of heterologous expression in *Escherichia coli* of *Pseudomonas aeruginosa* copper azurin. *Eur. J. Biochem.* 205:1123–1129.

Nar, H., A. Messerschmidt, R. Huber, M. van de Kamp, and G. W. Canters. 1992b. Crystal structure of *Pseudomonas aeruginosa* apo-azurin at 1.85 Å resolution. *FEBS Lett.* 306:119–124.

Pace, C. N. 1975. The stability of globular proteins. *CRC Crit. Rev. Biochem.* 3:1–43.

Plaxco, K. W., K. T. Simons, and D. Baker. 1998. Contact order, transition state placement and the refolding rates of single domain proteins. *J. Mol. Biol.* 277:985–994.

Pozdnyakova, I., J. Guidry, and P. Wittung-Stafshede. 2000. Copper triggered b-hairpin formation: initiation site for azurin folding? *J. Am. Chem. Soc.* 122:6337–6338.

Pozdnyakova, I., J. Guidry, and P. Wittung-Stafshede. 2001a. Copper stabilizes azurin by decreasing the unfolding rate. *Arch. Biochem. Biophys.* 390:146–148.

Pozdnyakova, I., J. Guidry, and P. Wittung-Stafshede. 2001b. Probing copper ligands in denatured *Pseudomonas aeruginosa* azurin: unfolding His117Gly and His46Gly mutants. *J. Biol. Inorg. Chem.* 6:182–188.

Schonbrunner, N., G. Pappenberger, M. Scharf, J. Engels, and T. Kiefhaber. 1997. Effect of preformed correct tertiary interactions on rapid two-state tendamistat folding: evidence for hairpins as initiation sites for beta- sheet formation. *Biochemistry.* 36:9057–9065.

Takano, K., J. Funahashi, Y. Yamagata, S. Fujii, and K. Yutani. 1997. Contribution of water molecules in the interior of a protein to the conformational stability. *J. Mol. Biol.* 274:132–142.

Tanford, C. 1970. Protein denaturation: C. Theoretical models for the mechanism of denaturation. *Adv. Protein. Chem.* 24:1–95.

van Pouderoyen, G., C. R. Andrew, T. M. Loehr, J. Sanders-Loehr, S. Mazumdar, H. A. Hill, and G. W. Canters. 1996. Spectroscopic and mechanistic studies of type-1 and type-2 copper sites in *Pseudomonas aeruginosa* azurin as obtained by addition of external ligands to mutant His46Gly. *Biochemistry.* 35:1397–1407.